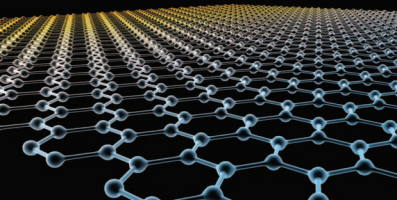


OXFORD

Graphene

A NEW PARADIGM IN CONDENSED MATTER
AND DEVICE PHYSICS

E. L. WOLF



Graphene

Graphene

*A New Paradigm in Condensed Matter
and Device Physics*

E. L. Wolf

Professor of Physics, Polytechnic Institute of New York University

OXFORD
UNIVERSITY PRESS

OXFORD
UNIVERSITY PRESS

Great Clarendon Street, Oxford, OX2 6DP,
United Kingdom

Oxford University Press is a department of the University of Oxford.
It furthers the University's objective of excellence in research, scholarship,
and education by publishing worldwide. Oxford is a registered trade mark of
Oxford University Press in the UK and in certain other countries

© E. L. Wolf 2014

The moral rights of the author have been asserted

First Edition published in 2014

Impression: 1

All rights reserved. No part of this publication may be reproduced, stored in
a retrieval system, or transmitted, in any form or by any means, without the
prior permission in writing of Oxford University Press, or as expressly permitted
by law, by licence or under terms agreed with the appropriate reprographics
rights organization. Enquiries concerning reproduction outside the scope of the
above should be sent to the Rights Department, Oxford University Press, at the
address above

You must not circulate this work in any other form
and you must impose this same condition on any acquirer

Published in the United States of America by Oxford University Press
198 Madison Avenue, New York, NY 10016, United States of America

British Library Cataloguing in Publication Data
Data available

Library of Congress Control Number: 2013940539

ISBN 978-0-19-964586-2

Printed and bound by
CPI Group (UK) Ltd, Croydon, CR0 4YY

Links to third party websites are provided by Oxford in good faith and
for information only. Oxford disclaims any responsibility for the materials
contained in any third party website referenced in this work.

Dedicated To
P. R. Wallace
G. W. Semenoff
A. K. Geim
K. S. Novoselov

Preface

Graphene, discovered in 2004 as a new phase of crystalline matter one atom thick, exhibits electronic conduction distinct from and superior to conventional metals and semiconductors and thus opens new opportunities for device design and fabrication. The single plane of graphite is now known to represent a new class of two-dimensional materials, one to several atoms in thickness that are conventionally crystalline in lateral dimensions micrometers to centimeters. The electrons in graphene move rapidly in a way that resembles massless photons and nearly massless neutrinos. They indeed exhibit Klein tunneling, a quantum phenomenon of unit probability specular tunneling through a high potential barrier that was originally conceived as a property of electrons and positrons in vacuum. These remarkable properties, endowed by the hexagonal “honeycomb” carbon-atom array onto ordinary electrons, fortunately are well explained by the methods of condensed matter physics, but that “explaining” has several initially puzzling aspects that we address.

This book is intended as such an explication: to introduce and simply explain what is so remarkably different about graphene. It describes the unusual physics of the material, that it offers linear rather than parabolic energy bands. The Dirac-like electron energy bands lead to high constant carrier speed, similar to light photons. The lattice symmetry further implies a two-component wave-function, which has a practical effect of cancelling direct backscattering of carriers. The resulting high carrier mobility allows observation of the quantum Hall effect at room temperature, unique to graphene. The material is two-dimensional, and in sizes micrometers to nearly meters displays great tensile strength but vanishing resistance to bending. We are intent as well to summarize the progress toward better samples and the prospects for important applications, mostly in electronic devices. The book is aimed at researchers and advanced undergraduate and beginning graduate students as well as interested professionals. This book is intended not as a text but a comprehensive summary and resource on a scientific and technological area of rapid advance and promise. The hope is to span the range between the painstaking small-science extraction from graphite of high quality graphene layers (that are, of course, part of every pencil lead) and high flying physics topics, including an anomalous integer quantum Hall effect at room temperature, bipolar transmission of Cooper pairs in a superconducting proximity effect, light-like charged particles only explainable by the Dirac equation, evidence for a unit-probability tunneling behavior (Klein tunneling) heretofore predicted, but never before observed. This book is also intended to suggest possibilities for new families of electron devices in a post-Moore’s Law version of nanoelectronics. Benzene rings, whose “radii” are about 0.190 nm, are excellent conductors (it is estimated that a screening current of ~ 3.9 nanoamperes/Tesla is estimated to flow around a benzene ring at room temperature) and might be viewed as basic units in graphene electronics.

Silicon and metal crystals lose their conductivity in small scale structures but the basic unit of graphene, essentially a benzene ring, still conducts well. A form of “chemistry” appears in the arrangement of broken bonds at the edges of graphene ribbons (e.g., terminations in zig-zag vs. armchair edges). A premium now is placed on experimental methods for epitaxial growths, from which a new “semiconductor technology” might arise. Device technologies that will necessarily depend on fabrication and patterning schemes for graphene layers are in a rapid state of development.

This book is dedicated to four physicists, two of them theorists and two experimentalists. P. R. Wallace first understood the unusual linear bandstructure in graphene (conceived as an approximation to graphite). G. W. Semenoff first understood the unusual two-sublattice origin of the chiral carriers, avoiding conventional backscattering and improving the mobility. A. K. Geim and K. S. Novoselov, two brilliant, resourceful and persistent experimentalists, showed how to isolate the individual planes and convincingly demonstrated their unique properties, indeed as representative of a new class of two-dimensional crystals.

The author is grateful to Sönke Adlung and Jessica White at Oxford University Press for invaluable help in conceiving and completing this project. It is a pleasure to acknowledge assistance from the Department of Applied Physics at NYU Poly, particularly from Prof Lorcan Folan and Ms. DeShane Lyew. Ankita Shah, Harsh Bhosale, Vijit Jain, Kiran Koduru and Manasa Medikonda, who have assisted with aspects of preparing the manuscript and clearing the way to publication. My wife Carol has helped in many ways and has been a constant source of support and encouragement.

E. L. Wolf, Brooklyn, New York, September, 2013

Contents

1 Introduction	1
1.1 “Crystals” one atom thick: a new paradigm	1
1.2 Roles of symmetry and topology	7
1.2.1 Linear bands, “massless Dirac” particles	7
1.2.2 “Pseudo-spins” from dual sublattices and helicity	11
1.3 Analogies to relativistic physics backed by experiment	14
1.4 Possibility of carbon ring electronics	17
1.5 Nobel Prize in Physics in 2010 to Andre K. Geim and Konstantin S. Novoselov	17
1.6 Perspective, scope and organization	18
2 Physics in two dimensions (2D)	20
2.1 Introduction	20
2.2 2D electrons on liquid helium and in semiconductors	21
2.3 The quantum Hall effect, unique to 2D	24
2.3.1 Hall effect at low magnetic field	25
2.3.2 High field effects	27
2.3.3 von Klitzing’s discovery of the quantized Hall effect	28
2.4 Formal theorems on 2D long-range order	32
2.4.1 Absolute vs. relative thermal motions in 2D	32
2.4.2 The Hohenberg–Landau–Mermin–Peierls–Wagner Theorem	38
2.4.3 2D vs. 2D embedded in 3D	39
2.4.4 Soft membrane, crumpling instability	40
2.5 Predictions against growth of 2D crystals	44
2.6 “Artificial” methods for creating 2D crystals	45
2.7 Elastic behavior of thin plates and ribbons	45
2.7.1 Strain Nomenclature and Energies	47
2.7.2 Curvature and Gaussian curvature	49
2.7.3 Isometric distortions of a soft inextensible membrane	50
2.7.4 Vibrations and waves on elastic sheets and ribbons of graphene	51
2.7.5 An excursion into one dimension	55
3 Carbon in atomic, molecular and crystalline (3D and 2D) forms	57
3.1 Atomic carbon C: $(1s)^2(2s)^2(2p)^2$	57
3.1.1. Wavefunctions for principal quantum numbers $n = 1$ and $n = 2$	58
3.1.2 Linear combinations of $n = 2$ wavefunctions	60

3.1.3	Two-electron states as relevant to covalent bonding	61
3.1.4	Pauli principle and filled states of the carbon atom	61
3.2	Molecular carbon: CH ₄ , C ₆ H ₆ , C ₆₀	63
3.2.1	Covalent bonding in simple molecules	63
3.2.2	Methane CH ₄ : tetrahedral bonding	67
3.2.3	Benzene C ₆ H ₆ : sp ² and π bonding	68
3.2.4	Fullerene C ₆₀	81
3.2.5	Graphane and Fluorographene	82
3.3	Crystals: diamond and graphite	83
3.3.1	Mined graphite	83
3.3.2	Synthetic “Kish” graphite	83
3.3.3	Synthetic HOPG: Highly Oriented Pyrolytic Graphite	84
4	Electron bands of graphene	86
4.1	Semimetal vs. conductor of relativistic electrons	86
4.2	Linear bands of Wallace and the anomalous neutral point	90
4.2.1	Pseudo-spin wavefunction	90
4.3	L. Pauling: graphene lattice with “1/3 double-bond character”	92
4.4	McClure: diamagnetism and zero-energy Landau level	92
4.5	Fermi level manipulation by chemical doping	93
4.6	Bilayer graphene	93
5	Sources and forms of graphene	98
5.1	Graphene single-crystals, flakes and cloths	98
5.1.1	Micro-mechanically cleaved graphite	98
5.1.2	Chemically and liquid-exfoliated graphite flakes	101
5.2	Epitaxially and catalytically grown crystal layers	108
5.2.1	Epitaxial growth on SiC: Si face vs. C face	109
5.2.2	Catalytic growth on Ni or Cu, with transfer	112
5.2.3	Large area roll-to-roll production of graphene	114
5.2.4	Grain structure of CVD graphene films	115
5.2.5	Hybrid boron-carbon-nitrogen BCN films	118
5.2.6	Atomic layer deposition	120
5.3	Graphene nanoribbons	121
5.3.1	Zigzag and armchair terminations	122
5.3.2	Energy gap at small ribbon width, transistor dynamic range	123
5.3.3	Chemical synthesis of perfect armchair nanoribbons	125
6	Experimental probes of graphene	128
6.1	Transport, angle-resolved photoemission spectroscopy	128
6.2	Optical, Raman effect, thermal conductivity	129
6.3	Scanning tunneling spectroscopy and potentiometry	132
6.4	Capacitance spectroscopy	133
6.5	Inverse compressibility with scanning single electron transistor (SSET)	136

7 Mechanical and physical properties of graphene	139
7.1 Experimental aspects of 2D graphene crystals	139
7.1.1 Classical (extrinsic) origin of ripples and wrinkles in monolayer graphene	141
7.1.2 Stability of graphene in supported samples up to 30 inches	146
7.1.3 Phonon dispersion in graphene	150
7.1.4 Experimental evidence of nanoscale roughness	158
7.1.5 Electrical conductivity of graphene in experiment	164
7.2 Theoretical approaches to “intrinsic corrugations”	169
7.3 Impermeable even to helium	176
7.4 Nanoelectromechanical resonators	178
7.5 Metal-insulator Mott–Anderson transition in ultrapure screened graphene	179
7.6 Absence of “intrinsic ripples” and “minimum conductivity” in graphene	183
8 Anomalous properties of graphene	185
8.1 Sublimation of graphite and “melting” of graphene	185
8.2 Electron and hole puddles, electrostatic doping and the “minimum conductivity”	191
8.3 Giant non-locality in transport	193
8.4 Anomalous integer and fractional quantum Hall effects	197
8.5 Absence of backscattering, carrier mobility	199
8.6 Proposed nematic phase transition in bilayer graphene	202
8.7 Klein tunneling, Dirac equation	204
8.8 Superconducting proximity effect, graphene Josephson junction	213
8.9 Quasi-Rydberg impurity states; Zitterbewegung	219
9 Applications of graphene	223
9.1 Transistor-like devices	224
9.1.1 High-frequency FET transistors	225
9.1.2 Vertically configured graphene tunneling FET devices	231
9.1.3 The graphene Barristor, a solid state triode device	237
9.2 Phototransistors, optical detectors and modulators	237
9.3 Wide area conductors, interconnects, solar cells, Li-ion batteries and hydrogen storage	244
9.3.1 Interconnects	248
9.3.2 Hydrogen storage, supercapacitors	249
9.4 Spintronic applications of graphene	251
9.5 Sensors of single molecules, “electronic nose”	254
9.6 Metrology, resistance standard	255
9.7 Memory elements	255
9.8 Prospects for graphene in new digital electronics beyond CMOS	257
9.8.1 Optimizing silicon FET switches	257

xii *Contents*

9.8.2	Potentially manufacturable graphene FET devices	263
9.8.3	Tunneling FET devices	264
9.8.4	Manufacturable graphene tunneling FET devices	266
10	Summary and assessment	270
	References	275
	Author Index	296
	Subject Index	301

1

Introduction

“Graphene” is the name given to a single-layer hexagonal lattice of carbon atoms, an extended two-dimensional lattice of benzene rings, devoid of hydrogen atoms. This one-atom-thick material has recently been found to be robust, if not completely planar, in samples tens of micrometers up to 30 inches in extent, on a supporting substrate. Graphene is a contender in the new information technology (and other) applications, beyond being a scientific breakthrough and curiosity. As we will see, electrons in graphene display properties similar to photons and neutrinos, never before observed in a condensed-matter environment. The new electron properties arise in a straightforward way from the symmetry of the atomic positions and the resulting cone-shaped, rather than parabolic, regions in the electron energy surfaces. It is reassuring to see that all the new effects are well described by the Schrödinger-equation-based methods of condensed matter physics that have served well in understanding solids from semiconductors to superconductors. Dirac-equation-like electron behavior in graphene is obtained directly from appropriate simplification of the Schrödinger theory of atoms, molecules and solids. Beyond this, graphene is the first example of a new class of two-dimensional crystals, a new phase of matter. This is a surprise in many ways that offers new opportunities, especially, in electronics.

The discovery of graphene extends, beyond some theoretical predictions, what useful forms matter can take. It is truly a new paradigm.

1.1 “Crystals” one atom thick: a new paradigm

A crystal is an ordered array of identical repeating units. We can think of the unit, in graphene, as the hexagonal benzene ring, whose diameter (between opposite carbon atoms, say those numbered 1 and 4) is $2a = 284$ pm,¹ where a is the carbon-carbon spacing (the 1–2 distance) $a = 142$ pm. Benzene, C_6H_6 , has one electron per atom binding a hydrogen atom at each ring location 1, 2, . . . to 6. In graphene, H is absent and that one electron per atom is delocalized over the whole crystal. The resulting perfectly ordered honeycomb lattice, for a $10\ \mu\text{m}$ sheet, is thus 35 211 benzene ring diameters (at 284 pm/ring) in linear size, certainly showing long-range order.

¹One picometer (pm) = 10^{-12} m. Common units on the atomic scale include Ångströms (10^{-10} m) and nanometers $1\text{nm} = 10^{-9}$ m. The Bohr radius of the hydrogen atom, also taken as the base unit of length on the atomic scale, is $a_0 = 0.0529$ nm.

2 Introduction

(Actually the lattice repeat distance, the “cell constant,” is the 1–3 distance in the ring, namely 246 pm.) And for the 30-inch sample the number of benzene ring diameters is 2.68 billion! (The corresponding two-dimensional honeycomb crystalline array will then certainly have defects, grain boundaries and dislocations, as are well known in conventional crystals.)

The honeycomb array in graphene is dictated by the facile three-fold planar bonding, via Schrödinger’s equation, of the quantum states of the carbon atom called 2s and 2p (discussed in Chapter 3). (One possibly might ask how honeybees chose the honeycomb lattice, composed of hexagons? Perhaps in the evolution of honeybees, the 3-fold lattice (that would put centers in all the hexagons) did not leave enough room for honey, and the cubic 4-fold lattice might collapse flat, like a cardboard box without the ends, squeezing the honey out.)²

In fact, the most economical description of the honeycomb lattice is that generated by fundamental translations of the *basis atoms* 1 and 2 (called A and B by physicists). This two-atom unit, when translated by \pm multiples of the translation vectors : $\mathbf{1}\rightarrow\mathbf{3}$, $\mathbf{1}\rightarrow\mathbf{5}$ gives the honeycomb lattice.³

The angle between these vectors is 60° , and we see that atoms 1, 3, 5 and 2, 4, 6 form triangles (they lie on the A and B sublattices, respectively), and that the two sublattices are separated by the interatomic vector $\mathbf{1}\rightarrow\mathbf{2}$. So the honeycomb lattice is fundamentally two interpenetrating triangular lattices, known as A and B. Thus *nearest-neighbor* atoms lie on *opposite* sublattices, with profound consequences in the unusual electronic bandstructure, as first recognized by the American physicist Wallace in 1947.

But the achieved 30-inch, one-atom-thick graphene sample certainly will be so floppy that it will have to be supported on some surface. This is the real question as to whether it is a crystal. If we imagine the honeycomb sheet as unsupported, we realize it is very susceptible to being bent out of its flat planar condition. The chemical bonds (“pi-bonds” = “ π -bonds” between two $2p_z$ electrons) will tend to return it to a flat planar condition, but this restoration force is weak. The large graphene sheet is very strong in tension, but weak against flexing motion. It is like a bedsheet, in being flexible but inextensible, but, unlike a bedsheet, it retains a weak restoring force toward a perfectly planar condition. We may italicize the word “crystal,” because inherent in two dimensions (2D) (embedded in three dimensional space) are long-wavelength flexural phonons that allow large root-mean-square (rms) fluctuational displacements, much larger than a lattice constant. How floppy the sheet will be depends on its size, as we will see shortly. It may be a matter of semantics whether a slightly bent crystal is still crystalline. From a familiar example: on a diving board, the deflections imposed by the diver’s weight exceed the cell dimension, but obviously do not suggest

²Why the honeybee evolution avoided 5-fold rings or tilings, all having unequal angles that do not permit an infinite crystal (but of course a honeycomb is finite), may have to do with eyes and brains better able to generate 120° angles, than the several angles in any 5-fold tiling.)

³A slightly different definition of the basis vectors as $\mathbf{1}\rightarrow\mathbf{3}$, $\mathbf{5}\rightarrow\mathbf{1}$ is given in Fig. 1.2b. In that choice, the angle between the basis vectors is 120° . Figure 4.1 shows the same choice of basis vectors as our present text.

collapse of the material supporting the diver. By formal definition, long-range order does not occur, but in practice the local distortions can be small, so that it is still useful to consider the sample as a crystal, if slightly distorted. For graphene in practice, the out-of-plane deflections are the main concern as to whether the system is crystalline.

But there is more, fortunately not of much practical importance, to the story of crystallinity in two dimensions. In addition, there are more subtle points, really only of academic interest that lead theorists to say that any 2D array, *even if arbitrarily kept absolutely planar*, cannot have long-range (infinite) order except at $T = 0$. (The planarity would have to be imposed without transverse pinning; the closest system of this type may be electron crystals on the surface of liquid helium.) We will discuss these points in Chapter 2, including a proof that an infinitely large 2D array would exhibit, at any finite temperature, large absolute in-plane motions (but without sensibly affecting local inter-atom distances). This might have a real effect, for example, in smearing the electron- or x-ray- diffraction spots on a sufficiently large sample, unless that sample was in effect pinned to be stationary at the measurement site. But since the phonon wavelengths (now in 2D) involved are large, local regions move *intact* so that local order is not disrupted. For example, the cohesive energy of the system is not reduced and this has nothing to do with the melting point of the system (that we connect with local order). In the words of Das Sarma (2011) “There is nothing mysterious or remarkable about having finite 2D crystals with quasi-long-range positional order at finite temperatures, which is what we have in 2D graphene flakes.” We return to this subject in Chapter 2, but simply comment here that the academic points in the literature do not in any way detract from the important potential uses of graphene in electronics and nano-electromechanical systems, as examples.

While there had been earlier suggestions that the single planes of graphite might be extracted for individual study (contrary to a theoretical literature that suggested that crystals in two dimensions should not be stable), Novoselov *et al.* (2004, 2005) were the first to demonstrate that such samples were viable, and indeed represented a new class of 2D materials with useful properties and potential applications. (Hints toward isolating single layers had earlier been given by Boehm *et al.* (1962), Van Bommel *et al.* (1975), Forbeaux *et al.* (1998) and Oshima *et al.* (2000), among others. And, as we will see in Section 5.1.2, chemists, since 1859, with notable work in 1898, have developed bulk processes to “exfoliate” graphite, as extracted from the ground, into “expanded,” typically oxidized, forms exposing, to a greater or lesser degree, the individual planes now called graphene.)

On small size scales, perhaps 10 nm to 10 μm , the graphene array of carbon atoms is “crystalline,” and has sufficient local order to provide electronic behavior as predicted by calculations based on an infinite 2D array. Micrometer-size samples of graphene show some of the best electron mobility values ever measured. In microscopy, on scales 10 nm to 1 μm , it sometimes may appear that the atoms are not entirely planar, but undulate slightly out of the plane. While it has been suggested that such “waves” are intrinsic (Morozov *et al.*, 2006), it is quite likely, on the contrary that they actually originate as the classical response of the thin membrane to inevitable stress from its

4 Introduction

mounting, or as a result of adsorbed molecules, since in graphene every carbon atom is exposed. Monolayer graphene is strong and continuous, but, because of its small thickness,⁴ $t \sim 0.34$ nm, all but the shortest samples are extremely “soft” in the sense of easily bending with a small transverse force. This can be understood from the classical “spring constant K ”⁵ for deflection x of a cantilever of width w , thickness t and length L (with Young’s modulus Y) under a transverse force F : $F = -Kx$. Since $K \sim Ywt^3/L^3$ (discussed in Section 7.4), with t near a single atom size, one sees that graphene, in spite of a large value of Young’s modulus, $Y \sim 1$ TPa, is the softest possible material against transverse deflection.

As we will see in Chapter 7, graphene rectangles, length L , width w and thickness t , quantitatively bend and vibrate as predicted by classical engineering formulas. For example, the spring constant K defined for deflection and applied force at the center of a rectangle clamped on two sides depends strongly on the dimensions as $K = 32Ywt^3/L^3$. A square of graphene, of size $L = w = 10$ nm, from the above formula, gives $K = 12.6$ N/m, while a square of size $10 \mu\text{m}$ has $K = 12.6 \times 10^{-6}$ N/m. If the sample is short, approaching atomic dimensions, the spring constant is large and the object appears to be rigid. For example, the spring constant of a graphene square ten benzene molecules on a side against bending can be estimated as ~ 156 N/m, using the formula, while the spring constant of a carbon monoxide (CO) molecule (in extension), deduced from its measured vibration at 64.3 THz, is known to be 1860 N/m. A further quantity in the graphene literature is Yt , a 2D rigidity that has a value of about 330 N/m. But for graphene longer than a few micrometers, with the spring constant K of a square falling off as $1/L^2$, the material is exceedingly soft.

Accordingly, graphene, on micrometer-size scales, conforms to any surface under the influence of attractive van der Waals forces. In an electron micrograph, graphene on a substrate appears adherent, more like a wet dishrag or “membrane” than a playing card, quite unlike a 10-inch diameter wafer of silicon. These 2D “crystals” cannot, at present, be grown from a melt, as is silicon and as were graphite and diamond in the depths of the earth at high temperature. Graphene crystals can only be obtained (see Chapter 5) by extraction from an existing crystal of graphite, or by being grown epitaxially on a suitable surface such as SiC or catalytically on Cu or Ni from a carbon-bearing gas such as methane.

⁴The space per layer in graphite is 0.34 nm that is widely quoted as the nominal thickness of the graphene layer. An equivalent elastic thickness of graphene, closer to the actual atomic thickness, is about 0.1 nm, see Section 2.7.

⁵The spring constant K is a macroscopic dimension-related engineering quantity quoted in SI units as N/m. It is related to the “bending rigidity” or “rigidity” $\kappa = Yt^3$, a microscopic property usually quoted in eV that is about 1 eV for graphene. (The Young’s modulus Y , an engineering quantity, is defined as pressure/(relative strain) = $P/(\delta x/x)$ and is about 10^{12} N/m² = 1 TPa for graphene, but see Section 2.7.1) The rigidity κ has units of energy, as force times distance. One sees that the rigidity κ of graphene, by virtue of the minimal atomic value of thickness t , is the lowest of any possible material. In connection with extension of a chemical bond, the spring constant K relates to the bond energy E as $K = d^2E/dx^2$.

Notably, graphene is an excellent electronic conductor, somewhat like a semimetal, but with conical rather than parabolic electron energy bands near the Fermi energy with a characteristic *linear* dependence of energy on crystal momentum, $k = p/\hbar$: i.e., $E = “pc” = c^*\hbar k$. These electrons move like photons, at speed $c^* \approx 10^6$ m/s and with vanishing effective mass. There is nothing magic about this; it simply results, in band theory, from the particular crystal lattice. This aspect also presents a new paradigm in the realm of condensed matter physics. Not only is Graphene nature’s closest approach to a two-dimensional (2D) self-supporting material, it also has charge carriers moving in a different way, as if their mass were zero. The physics of the situation also confirms that “back-scattering” is “forbidden” leading to measurably larger carrier mobility.

In the real world of atoms, no material can be mathematically two dimensional: the probability distribution $P(x,y,z)$ must extend in the z -direction by at least one Bohr radius. There are well-known examples of 2D subsystems of particles, notably electrons on the surface of liquid helium and the “2-DEG” two-dimensional electron gases engineered into leading semiconductor devices. The latter useful electron systems are supported by quantum well heterostructures. The remarkable difference, in graphene, is that there is no external supporting system, the layer of carbon atoms is the mechanical support, as well as the medium exhibiting light-like propagation of electrons. How is this possible?

The answer was not entirely clear before the discoveries of Geim and Novoselov: indeed the existence of free-standing graphene layers with novel electronic properties was a surprise, worthy of a Nobel Prize in Physics. Other one-layer materials include BN $(\text{BN})_n(\text{C}_2)_m$, with n, m , integers; MoS_2 , TaS_2 , NbSe_2 and the superconductor $\text{Bi}_2\text{Sr}_2\text{CaCu}_2\text{O}_x$, although the last is seven atoms thick (Novoselov *et al.*, 2005). So the Nobelists, in fact, confirmed the practical reality of a new class of 2D locally crystalline materials.

The binding energy of a crystal, an extended periodic array of atoms, for temperatures below a melting temperature, T_M , is a subject of solid state physics. The methods of this discipline do not always predict binding of an infinite 2D crystal. Indeed, thin layers of many substances are found to break up into “islands” as their thickness is reduced, especially if the attraction of atom to substrate exceeds the attraction atom-to-atom. This island breakup definitely does not occur with graphene: on the contrary, graphene is found to be among the strongest known materials under tension. Tenth-millimeter scale sheets of one-atom-thick graphene have been studied as elastic beams and sheets, whose vibrational frequencies have been measured consistent with a Young’s modulus ~ 1 TPa. At a lattice constant of 0.246 nm, a 20 μm graphene sheet (80 000 unit cells) looks flat, if suspended across a trench, but may bend in response to van der Waals forces from the mounting. In some cases, 10 nm-scale “waves” or “ripples” of ~ 1 nm amplitude have been inferred from transmission electron microscope measurements, with a likely origin in a combination of molecular surface adsorbates and mounting strain. Subtle physics is involved here, but experiments trump the situation; these “crystals” are large enough to be useful in many circumstances.

6 Introduction

Molecules have vibrations: in an extended crystal these are called phonons. The vibrational motions of molecules are 3D in nature and any real 2D crystal⁶ will have vibrational motion in the z -direction, termed flexural. In an extended real 2D sample the flexural motion extends to low frequency and large amplitude, at any finite temperature T . Even when restricted completely to planar motion, the methods of solid state physics have predicted that thermal vibrations at any finite temperature will lead to excessive transverse motion and destroy long-range (as distinct from short-range) order (Mermin and Wagner, 1966; Mermin, 1968). These theorems, it seems, do not prohibit (Das Sarma *et al.*, 2011) the observed finite size samples of graphene, although the theoretical predictions probably had a deterring effect on experimenters prior to the pioneers, Geim and Novoselov.

The benzene ring is planar, with restoring forces against bending. The two- and three-ring compounds naphthalene and anthracene, respectively, are also planar. We saw above that an effective spring constant $K \approx Ywt^3/L^3$ provides a useful estimate of the rigidity, depending on the length L . If graphene is an extended polymer of benzene rings, with the same 2s and 2p electrons (4 per atom) supporting the structure, it should similarly resist bending, tending to remain planar. Yet the resistance to bending is not so strong as to prevent rolled forms of graphene, including carbon nanotubes and scrolls (Braga *et al.*, 2004). An energy in favor of the 3D conformation is the sum of bonding energies of otherwise dangling or weakly satisfied bonds and of course, the van der Waals attraction that binds graphene layers into graphite. More stable states of carbon will clearly occur in 3D, where roughly there will be 6–8 nearest neighbors vs. 3 or 4 in a 2D configuration. A typical conformation of an extended micron-scale sheet of graphene laid onto a substrate is shown in Fig. 1.1. The behavior is that of a limp but nearly inextensible sheet, with wrinkles and conical cusps where there are singular elastic strains. It resembles a wrinkled sheet of paper, except that when removed from the substrate the wrinkles and conical cusps will disappear. The classical physics of this situation is described in Section 2.7.3 “Isometric distortions of a soft inextensible membrane”.

On size scales of tens to hundreds of micrometers, adequate for electronic devices, ambient temperature graphene is planar, exhibiting high carrier mobility. We will see later (Section 7.1.5) that removing adsorbates by heating to a modest temperature $\sim 400^\circ\text{C}$ can greatly improve the carrier mobility and electrical conductivity. There is some danger that unrecognized adsorbates have led to false impressions of “intrinsic” rippled behavior in graphene. We find that most small-scale non-planarity in the form of “corrugations” with lateral size scales of 10 to 100 nm with ~ 1 nm vertical amplitude, are the response of the nearly inextensible sheet to boundary conditions that inevitably introduce strain. The system will minimize the energy cost of the waves by maximizing their wavelength.

⁶A useful notation for a “real 2D crystal” is “2D-3” meaning that motion into the third dimension is available. A “pure” 2D system is one, like electrons on the surface of liquid helium, where no motion into the third dimension is allowed, the z -motion is represented by a single quantum state. We take the electron system inside graphene to be “pure 2D” as confined by the graphene lattice, even though that lattice may slightly undulate or flex into the third dimension.

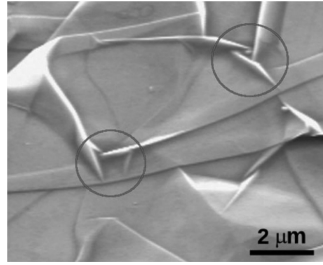


Fig. 1.1 Micrometer-scale transmission electron microscope (TEM) image of graphene sheet draped onto a substrate. It can be seen that the sheet is continuous but has little resistance to bending and folding. On a micrometer scale the single atomic layer, showing ripples with cusps or corners at their terminations, conforms to its supporting surface under the influence of van der Waals forces. Under tension it is very strong, with Young’s modulus on the order of 1 TPa. Only on a much smaller size scale can it be considered to be stiff or rigid against bending. (From Pereira *et al.*, 2010. © 2010 by the American Physical Society).

1.2 Roles of symmetry and topology

The interesting observed electronic properties of graphene are usefully predicted by theoretical solid state physics. The hexagonal honeycomb lattice, formally a triangular lattice with two atoms per unit cell (in 2D), leads to electronic bands in the usual way. In fact the electron bands, if not the subtle implications of their symmetry, were correctly predicted starting in 1947 (Wallace, 1947; McClure, 1956). The Brillouin zone is shown in Figs. 1.2a and 1.3b; the unit cell in Fig. 1.2b. A view of the lattice is again shown in Fig. 1.3a.

It is of extreme importance that A and B sublattices interpenetrate to form the honeycomb and the two sublattices, generated by the two atoms per unit cell, represent two separate groups of allowed states or bands. A carrier can be described by a two-component wavefunction, conveniently as if it had an “iso-spin” one-half that is not related to the physical spin of the electron.

1.2.1 Linear bands, “massless Dirac” particles

From an electronic band structure point of view, the essential novel feature is a set of linear electron bands: twin collinear intersecting vertical cones with apices at inequivalent corners \mathbf{K} , \mathbf{K}' of the hexagonal Brillouin zone. The Fermi energy lies near these degenerate intersection points in pure material, but E_F can be pulled up into the upper cones, making an n-type metal, or depressed into the lower cones, making a p-type metal, by an electric field (or by chemical doping). While the pure crystal at $T = 0$ has zero carriers, the material is typically observed to have finite conductivity, on the order of e^2/h . (With further work, this aspect has turned out to be an experimental artifact and a really pure and ordered sample is insulating at $T = 0$.) In

8 Introduction

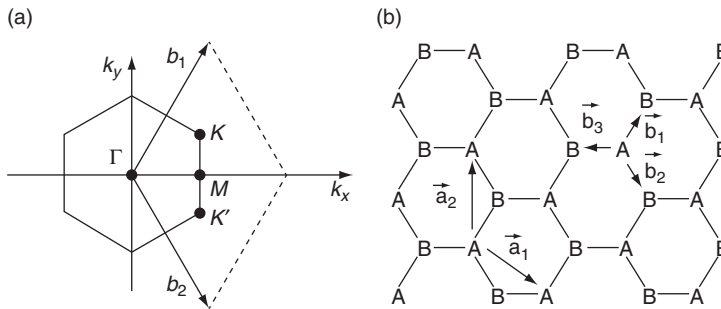


Fig. 1.2 (a) Hexagonal Brillouin zone of honeycomb lattice, resulting from A and B interpenetrating triangular lattices. If the nearest-neighbor distance is $a = 142$ pm, the lattice constant is $3^{1/2}a$ and the zone boundary M (half the reciprocal lattice vectors $\mathbf{b}_1, \mathbf{b}_2$), is $2\pi/3a$. The coordinates of the corner point K are $(2\pi/3a, \pi/3\sqrt{3}a)$ so that the distance from the origin to point K is $4\pi/(3\sqrt{3}a)$. Since the conduction and valence bands touch precisely at K, we have $k_F = |\mathbf{K}|$ and the Fermi wavelength $\lambda_F = 2\pi/k_F = 3\sqrt{3}a/2 = 369$ pm. (b) Honeycomb lattice, resulting from A and B interpenetrating triangular lattices. If the nearest-neighbor distance is $a = 142$ pm, the lattice constant is $3^{1/2}a = 246$ pm. The basis vectors of the triangular lattice are $\mathbf{a}_1 = (\sqrt{3}/2, -1/2)a$, $\mathbf{a}_2 = (0, 1)a$, and the sublattices are connected by $\mathbf{b}_1 = (1/2\sqrt{3}, 1/2)a$, $\mathbf{b}_2 = (1/2\sqrt{3}, -1/2)a$, $\mathbf{b}_3 = (-1/\sqrt{3}, 0)a$. (From Semenov, 1984. © 1984 by the American Physical Society).

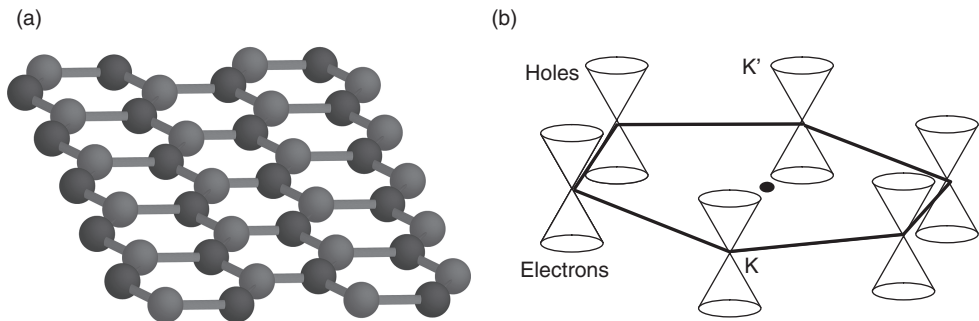


Fig. 1.3 (a) Honeycomb lattice emphasizing its composition as two interlocking triangular lattices. One may imagine the light shaded balls as the A lattice, the dark shaded balls as the B lattice. (b) Hexagonal Brillouin zone of honeycomb lattice, showing intersecting conical electron bands. The linear bands and the two “valleys” at K and K’ give unusual electronic properties to graphene. In a pure sample the lower cones are filled with electrons and the upper cones are empty.

experimental practice, the resistivity is typically less than $h/e^2 \sim 25 \text{ k}\Omega$ (Ohms per square [Ω/\square] in 2D).

This gives an aspect of a zero-band-gap semiconductor, except for the linear dispersion (Wallace, 1947). (This is in contrast to the usual case, as in Si and GaAs, where the electron bands have parabolic minima, leading to effective masses given by $m^* = \hbar^2/d^2E/dk^2$, with the result that carrier speeds vary linearly with crystal momentum, $k = p/\hbar$.) In this linear region for graphene, the particle velocity, $c^* = v_F = 3ta/(2\hbar)$ (Wallace, 1947; Katsnelson and Novoselov, 2007), is constant, entering light-like relations, $E = "pc" = c^*\hbar|\mathbf{k} - \mathbf{K}|$, valid near each "Dirac point". In this expression t is a nearest neighbor hopping energy, about 2.8 eV and a is the nearest-neighbor distance, 142 pm.

While the linear dispersion near the Fermi energy is novel for electrons, the calculation, including the speed c^* , is straightforward in the conventional, Schrödinger-equation-based, "tight-binding" method, using a nearest-neighbor hopping interaction t and bond length a . Taking t as 2.8 eV and $a = 142 \text{ pm}$, one finds $c^* = 0.91 \times 10^6 \text{ m/s}$, or about $c/300$. The connection between the linear dispersion and term "massless fermion" comes from the total energy formula of special relativity, $E = [(pc)^2 + (mc^2)^2]^{1/2}$ where the observed linear dependence $E = pc$ arises in the limit $m = 0$. The conical band structure, as mentioned, predicts zero conductivity for neutral graphene with the Fermi energy at the Dirac point where the density of states vanishes. Clearly, because (at zero temperature) "undoped graphene has no free electrons, an infinite sample cannot conduct electricity," as stated by Snyman and Beenakker (2007).

Experiments (Novoselov *et al.*, 2004) showed that the electrical conductivity as a function of charge density of graphene rises symmetrically on either side of a minimum at the neutrality point. In the experiment, a gate applied electric fields to induce charge of either sign, much as in a field-effect transistor. The sharp peak in resistivity at the crossing point, and other features, are confirmed by Zhang *et al.* (2005), as shown in Fig. 1.4.

As indicated in Fig. 1.4, the mobility in graphene rises as the carrier concentration falls, and values as high as $200\,000 \text{ cm}^2/\text{Vs} = 20 \text{ m}^2/\text{Vs}$ have been obtained in suspended samples (Bolotin *et al.*, 2008).

While the mobility is clearly sample dependent, the maximum resistivity values near $h/4e^2 \approx 6.45 \text{ k}\Omega$, were initially suggestive of a quantum condition, catalogued by Novoselov *et al.* (2005) as shown in Fig. 1.5, a bit larger than the $\sim 4 \text{ k}\Omega$ shown in Fig. 1.4. The exact formula for the quantum limit was still discussed until 2011. The leading theoretical value, $h/4\pi e^2$, seems small by a factor of π , but is in disagreement with a basic paper (Abrahams *et al.*, 1979) that predicts an infinitely large resistivity at zero temperature.

It is now believed that the "minimum conductivity," a practical matter in dealing with graphene, is actually an artifact of extrinsic electron and hole "puddles," for which similar theoretical conductivity estimates can be found, on the basis of percolation and tunneling between adjacent puddles. An early indication of this non-metallic behavior was offered by Bolotin *et al.* (2008) who described "a nonuniversal conductivity that

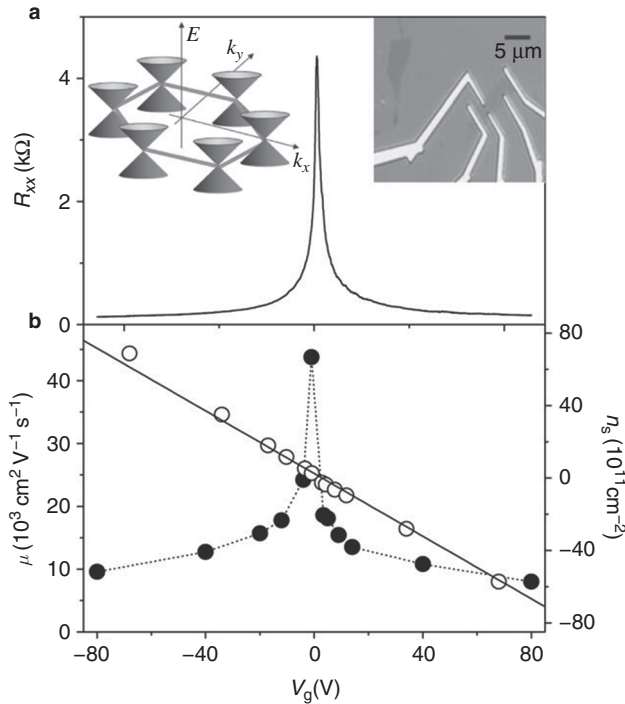


Fig. 1.4 Electric field effect in single-layer graphene obtained by variation of voltage V_g on gate underlying the sample (see the upper right inset). (a) A resistance maximum about 4 k Ω is seen here at 1.7 K at gate voltage corresponding to the neutrality point, where Fermi level drops to the apices shown in upper left inset. (b) The carrier density n , shown as open circles, from a Hall measurement, and the mobility are plotted. The mobility, on the order of 4 m²/Vs at peak, implies a long mean free path $\lambda \sim 1$ μm . The line in lower panel, well matching the measured carrier density points, comes from an estimate of the charge induced by the gate voltage, $n = C_g V_g / e$, where $C_g = 115 \text{ aF}/(\mu\text{m})^2$ is obtained from the geometry. (From Zhang *et al.*, 2005, by permission from Macmillan Publishers Ltd., © 2005).

decreases with decreasing T,” after applying a heating procedure to their 4-point-probed graphene sample to remove adsorbed impurities. The simple cleaning procedure was found to increase the conductivity by about a factor of 10. Surface scattering is thus a factor in much of the literature before 2008, for example, in the earlier work in the Kim group, Tan *et al.* (2007).

A recent experiment on screened graphene which succeeded in nearly removing the “puddles,” reveals what appears to be a conventional Mott–Anderson transition to an insulating state at low temperature, shown in Fig. 1.6.

These new results are revealed by Ponomarenko *et al.* (2011) in a paper entitled “Tunable metal-insulator transition in double-layer graphene heterostructures”. The

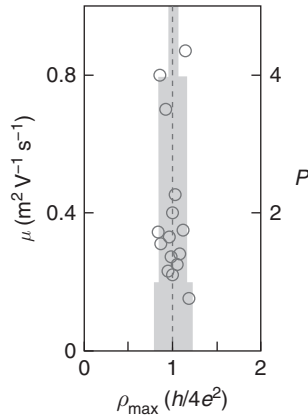


Fig. 1.5 Maximum values of resistivity ρ_{\max} (circles) exhibited by devices with mobilities (left y axis). Histogram in darker shade shows the number of devices P exhibiting ρ_{\max} within 10% intervals around the average value $\sim h/4e^2$. Bolotin *et al.* (2008) found that mobilities about a factor of 10 larger were easily available by gently heating the samples to release adsorbed gases that evidently strongly scatter charge carriers. (From Novoselov *et al.*, 2005, by permission from Macmillan Publishers Ltd., © 2005).

tuning is of the carrier concentration in the graphene layer intervening between the (puddle-inducing) substrate, containing charged impurities, and the measured graphene layer. The two graphene layers are separated by $d = 12$ nm and the concentration in the screening layer is $3 \times 10^{11} \text{ cm}^{-2}$. The 12 nm spacing is large enough that the measured graphene layer does not exchange carriers with the screening layer: more details are contained in Section 7.5. (A tunneling FET configuration is attainable at smaller spacings d , as will be described in Chapter 9.)

These features are in accord with the band diagram in Fig. 1.3 and the upper left inset to Fig. 1.4 and are further discussed in Section 7.5. But there are further unusual aspects of graphene, subtle but important, due to the dual sublattices arising from the two atoms per unit cell that we now discuss.

1.2.2 “Pseudo-spins” from dual sublattices and helicity

The need for a two-component or “pseudo-spin” electron wavefunction near these “Dirac points” was more recently realized (DiVincenzo and Mele, 1984; Semenoff, 1984; Novoselov, *et al.*, 2004, 2005, 2006, 2007). These workers showed that the double-sublattice origin of the states in the cones \mathbf{K} , \mathbf{K}' requires such a treatment, based on a “pseudo-spin” of lattice origin. Semenoff described the graphene Brillouin zone as having two “right- and left-handed degeneracy points” (where valence and conduction bands meet). In each hexagonal ring, three atoms are in the A lattice and three atoms are in the B lattice, as we have seen. (We will return to the band structure of graphene

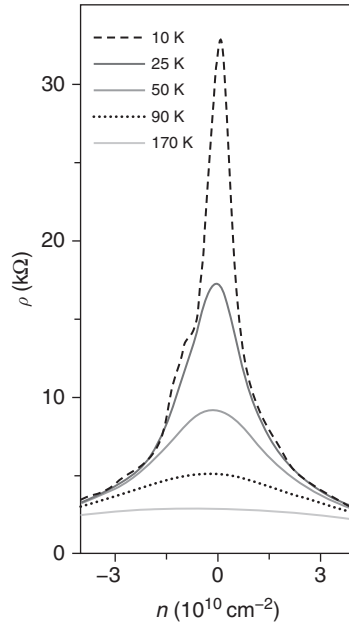


Fig. 1.6 Maximum value of resistivity more recently measured is in fact strongly temperature dependent, and reaches 33 kΩ (about $5.12 h/4e^2$, well above the Anderson localization value) at 10 K. This is now regarded as intrinsic behavior, attained by screening away extrinsic potential fluctuations that supported “puddles” of locally high and conducting electron and hole concentrations, now recognized as subtle artifacts. The authors describe the curves in Fig. 1.6 as exhibiting an “insulating temperature dependence”. This is a device of the type shown in Fig. 7.31a with BN spacer 12 nm and screening layer concentration $3 \times 10^{11} \text{ cm}^{-2}$. (From Ponomarenko *et al.*, 2011, by permission from Macmillan Publishers Ltd., © 2011).

in Chapter 4.) The tight-binding Hamiltonian used is of the simplest form, allowing only nearest-neighbor interactions $t(a_i^* b_j + b_i^* a_j)$ (on opposite sublattices) plus second-nearest-neighbor interactions (same sublattice): $t'(a_i^* a_j + b_i^* b_j)$.⁷

By the symmetry of the lattice, the Schrödinger theory expression simplifies into a Dirac-like form giving conical bands.

In this range of energies, $|E| \lesssim 1 \text{ eV}$, the Hamiltonian for the single-layer electron system, making use of the “tight binding” and “ $\mathbf{k} \cdot \mathbf{p}$ ” approximations, widely used in semiconductor physics (Yu and Cardona, 2010; Semenoff 1984), reduces to the matrix form

$$\hat{H} = \hbar c^* \begin{pmatrix} 0 & k_x - ik_y \\ k_x + ik_y & 0 \end{pmatrix} = \hbar c^* \boldsymbol{\sigma} \cdot \mathbf{k} \quad (1.1)$$

⁷In such expressions, a_i^* (a_i) represent operators that create (destroy) an electron on site i .

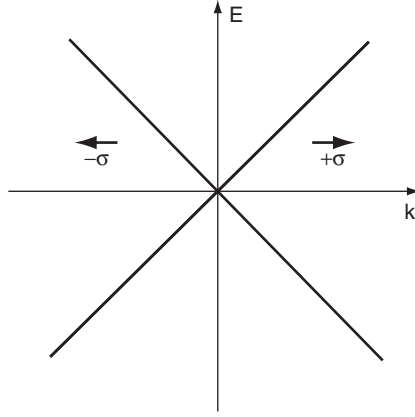


Fig. 1.7 Model energy dispersion $E = \hbar c^* |k|$ at each Dirac point. The ascending line arises from one sublattice, the descending line from the other, suggesting that transitions between branches are “spin-forbidden”. Back-scattering is thus reduced, making the quantum Hall effect observable even at room temperature.

where \mathbf{k} is the quasiparticle momentum and $\boldsymbol{\sigma}$ the two-dimensional Pauli matrix. This reduction of the Hamiltonian into a form similar to the Dirac equation for massless particles comes from the crystal symmetry and the two equivalent sublattices A and B. The cosine-like energy bands (each C atom has one participating $2p_z$ valence electron that form π^* anti-bonding bands at positive energy and π bonding bands at negative energy) intersect in the cones at the six corners of the Brillouin zone. That the electronic states arise from two (A and B) triangular sublattices leads, as mentioned above, to a two-component wavefunction (Semenoff, 1984) mathematically treated as spin $1/2$. The Pauli matrix $\boldsymbol{\sigma}$ here refers to the *pseudo-spin*, not to the actual electron spin that is neglected at this point. These features only appear near the degeneracy (Dirac) points, where their importance is clear from measurements on graphene.

The wavefunction that is needed near the Dirac point \mathbf{K}' can be written (Kane and Mele, 1997; Castro Neto *et al.*, 2009) as

$$\psi_{\pm, \mathbf{K}'}(\mathbf{k}) = \frac{1}{\sqrt{2}} \begin{pmatrix} e^{i\theta_{\mathbf{k}}/2} \\ \pm e^{-i\theta_{\mathbf{k}}/2} \end{pmatrix} \quad (1.2)$$

$$\theta_{\mathbf{q}} = \arctan \left(\frac{q_x}{q_y} \right) \quad (1.3)$$

for π^* states above (+) and π states (−) below the Fermi energy. Here \mathbf{q} is the momentum measured from the Dirac point \mathbf{K}' , and the angle θ is measured around that point. Similar equations apply for point \mathbf{K} , with the opposite choice of \pm sign in

eqn (1.2), to reverse the helicity. In both cases, the two components of the wavefunction indicate the separate contributions from the separate sublattices, A and B. Thus one may say that each π -electron carries, in addition to its physical spin and momentum, an internal pseudo-spin index, labeling the sublattice state, and a further “pseudo-spin” index, labeling the two independent Dirac spectra derived from the \mathbf{K} and \mathbf{K}' points in the Brillouin zone.

The *pseudo-spin* of the particle, in relation to its motion, gives rise to helicity or chirality. Helicity is the projection of spin $\boldsymbol{\sigma}$ onto the direction of motion \mathbf{k} and is positive (negative) for electrons (holes) defined as:

$$h = 1/2 \boldsymbol{\sigma} \cdot \mathbf{p}/|\mathbf{p}| \quad (1.4)$$

The concept of helicity is valid near the Fermi energy and to the extent that second-nearest-neighbor interactions are negligible. Its relevance is confirmed by observation of anomalous quantum Hall effects in graphene. Further, the long, micrometer-scale, mean free paths seen in metallic carbon nanotubes (McEuen *et al.*, 1999) have been related to cancellation of backscattering of chiral electrons within a given valley (see Section 8.4). The reversal of k_x to $-k_x$, because of the chirality, involves a rotation of the pseudo-spin (that always points in the direction of motion). But the reversal of the pseudo-spin is forbidden because the electronic wavefunctions of the A and B sublattice contributions are orthogonal. We will return to this topic in Chapter 8.

As an alternative narrative, the “spin” part of the wavefunction eqn (1.2) has half-angles, so that, if the particle executes a closed path, with angle θ gaining 2π , as it might in returning from a scattering center, the wavefunction phase advances by $\theta/2$, an angle π , leading to a minus sign and cancellation of backscattering.

The electron states, finally, have 4-fold degeneracy, including the valley (\mathbf{K} , \mathbf{K}') degeneracy and the electron spin degeneracy. The density of states per unit cell is $g(E) = 2 A_C |E| / (\pi \hbar^2 v_F^2)$, where $v_F = c^*$ and $A_C = 3\sqrt{3} a^2/2$ is the cell area, with a the nearest-neighbor distance. (See also eqn (4.13), and related text.)

1.3 Analogies to relativistic physics backed by experiment

A 2D electron system in a perpendicular magnetic field gives rise to Landau levels (LL) whose energies conventionally are $E = (n + 1/2) (eB\hbar/m)$, with $n = 0, 1, 2, \dots$ and m the electron mass. The minimum energy in this set is $1/2 \hbar\omega_c$, where the cyclotron frequency is $\omega_c = eB/m$. (We use SI units, note that much of the theoretical literature on graphene and quantum Hall effect uses cgs (centimeter-gram-second) units, where the cyclotron frequency would be written as eB/mc .) For a system of area A , the total number of orbital states at the LL energy is $N = AB/\varphi_0$, where $\varphi_0 = h/e$ is the (one electron) magnetic flux quantum. The quantum Hall effect occurs when N is similar to the total number of mobile electrons in the system so that “all electrons are in fully quantized states”. This effect is only present in two-dimensional 2D systems, as will be discussed in Chapter 2. (The quantum Hall effect is observable in graphene even at room temperature, as we will see in Section 8.3, because of the exceptionally large mean free

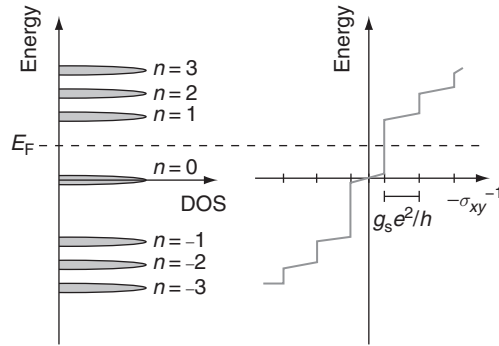


Fig. 1.8 Anomalous quantum Hall effect (QHE) in monolayer graphene shows a Landau level at zero energy [corresponding to central peak in density of states (DOS)]. This anomalous observation is the signature of the massless Dirac Fermion. The conventional QHE has a gap at zero energy. The measured quantity on the right, contrary to the label, is $-\sigma_{xy} \approx R_{xy}^{-1}$ that conventionally rises by $g_s e^2/h$, with g_s the spin degeneracy, as a Landau level crosses the Fermi energy. (From Zhang *et al.*, 2005, by permission from Macmillan Publishers Ltd., © 2005).

path.) The graphene LL spectrum is anomalous, including a prominent level at zero energy that supports the pseudo-spin wavefunction. The anomalous observed levels can be written (Novoselov, 2011) as

$$E_n = \pm v_F [2e\hbar B(n + 1/2 \pm 1/2)]^{1/2} \quad \text{where } n = 0, 1, 2, \dots \quad (1.5)$$

In this expression, describing a half-integer quantum Hall effect, the $\pm 1/2$ term is related to the chirality of the quasiparticles and ensures the existence of two energy levels (one electron-like and one hole-like) at exactly zero energy, each with degeneracy half that of all other Landau levels (McClure, 1956, 1960).

The data of Zhang *et al.* (2005) are shown in Fig. 1.8 (very similar data were reported on p. 197 of the same journal by Novoselov *et al.* [2005]). We will return to this topic later (in Section 8.3), in the book.

The spacing of the Landau levels shown in Fig. 1.8 is similar to that predicted for massless Dirac electrons (as measured by a scanning single electron transistor) shown in Fig. 1.9a and directly observed by Miller *et al.* (2009) in scanning tunneling spectroscopy, in Fig. 1.9b.

The data in Fig. 1.9a are due to Martin *et al.* (2009), using a scanning single electron transistor (SSET, described in Chapter 6) to locally measure what is called the “inverse compressibility” of the electron system.⁸

⁸The measured quantity is $d\mu/dn$ where μ is the chemical potential and n is the density of carriers.

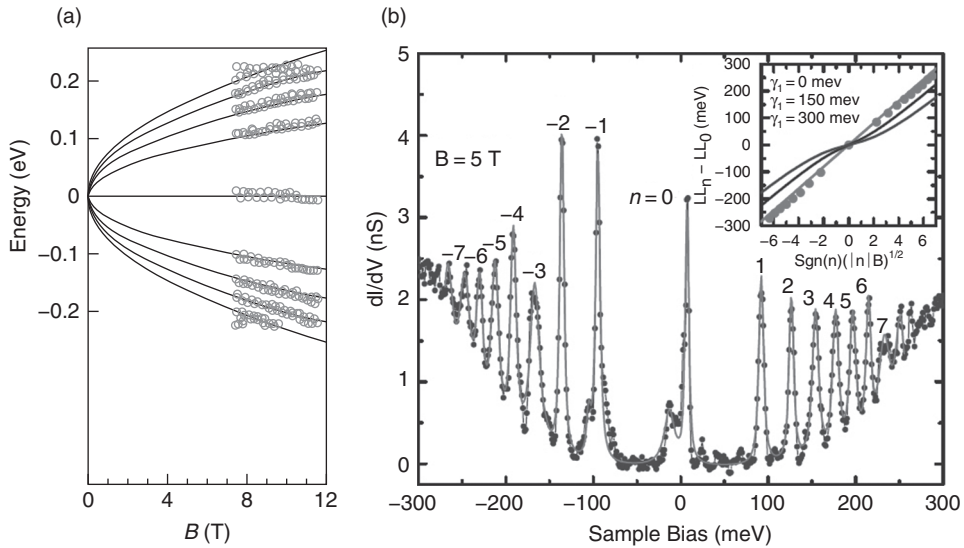


Fig. 1.9 (a) The observed anomalous $B^{1/2}$ energy dependence of Landau levels, contrary to the usual linear dependence, is strong evidence that the electron carriers in graphene behave as “massless Dirac fermions,” because of the unusual lattice symmetry. The conventional formula $\omega = eB/m$ is untenable for m essentially zero. Measurements by method of scanning Single Electron Transistor (SET) by Martin *et al.* (2009). (This measurement method will be mentioned in Chapter 6.) (Martin *et al.*, 2009, Fig. 1). (From Martin *et al.*, 2009, by permission from Macmillan Publishers Ltd., © 2009) (b) The observed anomalous $B^{1/2}$ energy dependence of Landau levels, as well as the zero-energy Landau level, are clearly seen in Scanning Tunneling Spectroscopy. (From Miller *et al.*, 2009, with permission from AAAS).

The data are obtained at 11.7 T with the scanning SET tip hovering “a few tens of nanometers” above the monolayer graphene, supported on the conventional oxidized silicon wafer. The indexing used by Martin *et al.* (2009) for the Landau levels is

$$E_i = \text{sgn}(i) [2e\hbar v_F^2 |i| B]^{1/2} \quad (1.6)$$

with integer i running from $i = -4$ to $i = +4$. Positive i values indicate electron-like Landau levels, and negative i values indicate hole-like Landau levels. The solid lines are calculated on this formula using the best fit value $v_F = 1.1 \times 10^6$ m/s that the authors say is ten percent higher than the theoretical estimate. The anomalous zero-energy Landau level is prominent.

To summarize, the Landau level spectrum of graphene is doubly anomalous, first in the presence of the zero-energy peak and second in the uneven spacing of the levels, represented by the square-root factor in eqn (1.5).

1.4 Possibility of carbon ring electronics

Transistors can be made from single-layer carbon films, a saving in material costs for a start. One does not have to grow a large crystal and saw it into wafers, although it is true that an epitaxial substrate such as SiC may still be needed. The mobility of the carriers is exceptionally high, translating into the chance for a ballistic device working at room temperature. Further, the mobility remains high even for high carrier concentrations. The valley degeneracy and spinor property prohibiting backscattering offer new avenues for making devices. The drawback that one sees at the outset is that graphene does not have a high resistivity state, so On/Off ratios in a conventional FET configuration are limited. Patterning graphene into nanoribbons, with space quantization of levels across the ribbon, offers the chance to introduce energy barriers, even though in some situations anomalous Klein tunneling of carriers is expected. Patterning is itself a major, if not impossible, challenge, on the size scale of a benzene ring, as is potentially available. The details of the patterned edge, whether it is “armchair” or “zigzag” in the notation of carbon nanotubes, significantly affect the electrical properties. How the unpaired electrons at the “broken bonds” are passivated may also be an important aspect. The graphene sheet can, in principle, be patterned to act as a single electron transistor (SET) as well as a field-effect transistor, and indeed on a molecular scale. As we will see in Chapter 9, activity in these directions is occurring at leading firms. There is no question that graphene elements will play important supplemental roles in the silicon chip industry. A more realistic and detailed account of graphene field-effect FET transistors, including a possible family of graphene tunneling T-FET switching devices is given in Chapter 9, especially Section 9.8.

1.5 Nobel Prize in Physics in 2010 to Andre K. Geim and Konstantin S. Novoselov

The 2010 Nobel Prize in Physics was shared by Andre K. Geim and Konstantin S. Novoselov for their work on graphene. They had isolated and named the single layers in 2004. The method that they used, basically using Scotch tape to pull the graphite apart, was simple and accessible, and provided samples still the best available. This caused a rush of new experiments. Graphene, as they showed, was really only one example of a class of two-dimensional crystals that they had discovered. Their experimental work revealed the remarkable electronic properties of graphene, and they tied these to earlier work in relativistic particle physics. The material itself has unique and superior properties, both mechanically and electrically, and has many possible applications. The explosion of publications related to graphene has been truly remarkable. A very recent review of the rapidly expanding literature and assessment of applications is given by Novoselov *et al.* (2012).

The Nobel Lectures are: Andre K. Geim (2011), “Random Walk to Graphene” and K. S. Novoselov (2011), “Graphene: Materials in the Flatland”. These are excellent sources of information including references up to 2010. The citation for the Nobel Prize mentions “groundbreaking experiments regarding the two-dimensional material graphene.” An added source of information is “Scientific Background on the

Nobel Prize in Physics 2010: Graphene” compiled by the Class for Physics of the Royal Swedish Academy of Sciences. The two physicists have been knighted by Queen Elizabeth II in the UK.

1.6 Perspective, scope and organization

The discovery of 2004 has led to an explosion of literature on graphene and to a lesser extent on the class of 2D crystalline systems.

The brilliant experimental work has revealed a vast amount of new information. Experimental work on graphene is very difficult because every carbon atom is exposed to the environment that contains contaminating atoms and molecules, and also stray electric fields that have the effect of inducing charge carriers in the graphene. The new field has gone through phases where effects were seen repeatedly and thought to be fundamental when, in light of improving methods and sample quality, the effects were later realized as consequences of contaminants, mounting strains or stray electric fields. The field has also appeared more mysterious than it really is by the uncertain relevance of the theoretical literature on the limitations of crystalline order in two dimensions. The other mysterious behaviors, analogies between the electrons in graphene and photons and neutrinos in high energy physics are confirmed and explained by the brilliant experiments including observation of the Klein tunneling effect, to make graphene indeed an interesting material.

This book undertakes to systematically review all of the work, taking seriously even those aspects that now appear less urgently relevant. We cover in Chapter 2 all of the literature on 2D systems, theoretical and experimental. The theoretical literature has two branches, one devoted to ideal 2D arrays with no motion allowed into the third dimension, where excessive in-plane thermal motion, described by logarithmic divergences in atomic excursions from lattice sites, are correctly predicted at finite temperature, but have not been seen in experiment. Purely 2D systems, before discovery of the free electron subsystem contained in graphene, were realized experimentally as electrons on the surface of liquid helium and electrons in the quantum Hall effect. We review the quantum Hall effect, as it was a key to understanding 2D electron behavior in graphene. In the second branch of 2D that we can refer to as 2D-3, a planar system, like graphene, can distort into the third dimension. A large literature here comes from polymer work, and the central question has often been whether or how the 2D system (“membrane”) may “crumple” at high temperature, in such a way that an initially flat system of area L^2 eventually fills a volume of size up to L^3 . Mechanical engineering also understands 2D-3 systems in the context of bending beams and plates, and it appears that these descriptions are actually more applicable to graphene than are the polymer-related treatments. In the end it appears that graphene does not in fact crumple, but disintegrates near 4900 K. Graphene, suggested as unstable, certainly seems to exist at least to 3900 K, the measured sublimation temperature of graphite.

In Chapters 3, 4 and 5 we deal, respectively, with properties of carbon as atoms, molecules (with attention to benzene rings), and in its solid forms; with the electron

bandstructure of mono-layer and bi-layer graphene; and with the sources and types of graphene, ribbons and bilayers. Chapter 6 introduces several of the less-familiar experimental methods that have been helpful in understanding graphene, including angle-resolved photoemission spectroscopy (ARPES), electron scanning tunneling microscopy and spectroscopy (STM, STS) and the scanning single-electron transistor (SSET). Chapter 7 is a review of the physical properties of graphene, with attention to the lattice stability of the material as affected by the flexural modes of vibration well studied by neutron diffraction and other methods. The question of undulations and waves is examined, from the view of experiment and the view of theory, leading to the suggestion that the effects are subtle responses of the atomically thin system to typical environments including gaseous contamination and strain introduced by a mounting structure. Chapter 8 describes several areas of graphene behavior that can be regarded as anomalous, including the predicted disintegration at 4900 K primarily into linear chain fragments of carbon moving away into space. This chapter also covers the Klein tunneling discovery, recent results in the quantum Hall effect, discovery of non-local behavior and work suggesting a nematic phase transition of the electron system. Chapter 9 is devoted to applications of graphene. The emphasis is on electronic devices with particular attention to transistors, including radio-frequency (100 GHz) transistors, flash memory elements, optical devices and the interesting questions relating to a possible new class of switching transistors that can be miniaturized beyond the limits of Moore's Law as it applies to silicon. Finally, emphasis is on types of graphene transistors that are potentially manufacturable in existing technology and that will operate as switches in spite of the essentially semi-metallic nature of graphene. Chapter 10 is a summary and assessment, with attention to key questions of expanding methods to obtain high quality samples for electronic applications at reasonable cost. Briefly it is suggested that the primary advantage of graphene in device applications is the continuity and high conductivity available literally down to a thickness of one atom.